Dalton Transactions

ROYAL SOCIETY OF CHEMISTRY

PAPER

View Article Online
View Journal

Cite this: DOI: 10.1039/d0dt01935f

Quinoline-triazole half-sandwich iridium(III) complexes: synthesis, antiplasmodial activity and preliminary transfer hydrogenation studies†

Diana R. Melis,[a] Christopher B. Barnett,[a] Lubbe Wiesner,[b] Ebbe Nordlander[c] and Gregory S. Smith *[a]

Received 29th May 2020,
Accepted 15th July 2020

DOI: 10.1039/d0dt01935f

rsc.li/dalton

Iridium(III) half-sandwich complexes containing 7-chloroquinoline-1,2,3-triazole hybrid ligands were synthesised and their inhibitory activities evaluated against the *Plasmodium falciparum* malaria parasite. Supporting computational analysis revealed that metal coordination to the quinoline nitrogen occurs first, forming a kinetic product that, upon heating over time, forms a more stable cyclometallated thermodynamic product. Single crystal X-ray diffraction confirmed the proposed molecular structures of both isolated kinetic and thermodynamic products. Complexation with iridium significantly enhances the *in vitro* activity of selected ligands against the chloroquine-sensitive (NF54) *Plasmodium falciparum* strain, with selected complexes being over one hundred times more active than their respective ligands. No cross-resistance was observed in the chloroquine-resistant (K1) strain. No cytotoxicity was observed for selected complexes tested against the mammalian Chinese Hamster Ovarian (CHO) cell line. In addition, speed-of-action assays and β-haematin inhibition studies were performed. Through preliminary qualitative and quantitative cell-free experiments, it was found that the two most active neutral, cyclometallated complexes can act as transfer hydrogenation catalysts, by reducing β-nicotinamide adenine dinucleotide (NAD^+) to NADH in the presence of a hydrogen source, sodium formate.

Introduction

Malaria, a life-threatening mosquito-borne blood disease caused by parasites of the *Plasmodium* genus, poses an enormous challenge to world health.[1] This challenge is highlighted by the staggering annual infection and mortality rates, making it clear why combating this disease, which affects predominantly the poorest countries in the world, is of great importance.[2] The oldest and most well-known class of antimalarial drugs are those containing the heterocyclic aromatic quinoline moiety, including chloroquine (CQ), a drug that has been the mainstay of malaria treatment for decades and is still used in combination treatments for this disease.[3,4] The emergence and spread of CQ-resistant strains of malaria, however, has become a major problem, leading to the need to develop novel and effective antimalarials that are chemically and structurally diverse.[5,6] The World Health Organisation now recommends artemisinin-based combination therapies (ACTs) as the frontline treatment for malaria caused by *P. falciparum*, the most deadly of malaria parasites.[5,7–9] They too, however, are beginning to lose their efficacy as artemisinin-resistant strains of the malaria parasite have begun to emerge in Southeast Asia.[10] It is, therefore, necessary to continue to develop novel antimalarial therapies in order to manage a disease of this magnitude.

Owing to its favourable biopharmaceutical properties, as well as its safety and cost effectiveness, newer strategies aimed at modifying chloroquine to overcome resistance are attractive.[11,12] A 2019 review by Chu *et al.* details some of the recent advances in the use of quinoline-triazole hybrids as potential antiplasmodial and antimalarial agents.[13] Triazoles are particularly desirable pharmacophores as they are stable to acid–base hydrolysis, relatively resistant to metabolic degradation and readily associate with biological targets *via* hydrogen bonding.[14–18] Although the quinoline-triazole hybrids were mostly found to have moderate, micromolar antiplasmodial activity, this activity might be improved by the incorporation of a metal into their structure, a method of derivatisation

[a]*Department of Chemistry, University of Cape Town, Rondebosch, Cape Town, South Africa. E-mail: gregory.smith@uct.ac.za*
[b]*Division of Clinical Pharmacology, Department of Medicine, University of Cape Town, Observatory 7925, Cape Town, South Africa*
[c]*Chemical Physics, Department of Chemistry, Lund University, Box 124, SE-221 00 Lund, Sweden*

†Electronic supplementary information (ESI) available. CCDC 2003818 (**3a**) and 2003819 (**4**). For ESI and crystallographic data in CIF or other electronic format see DOI: 10.1039/d0dt01935f

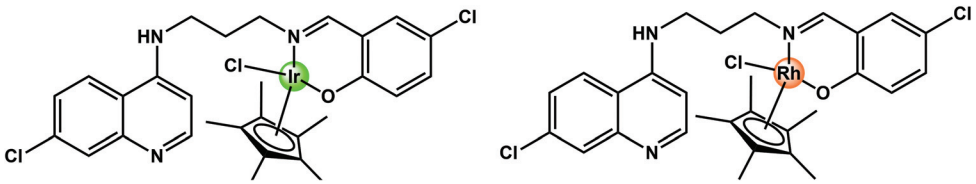

Fig. 1 Quinoline complexes investigated in the study by Stringer *et al.*[40]

which has recently become popular. Fuelled by the success of the platinum-based anticancer drug, cisplatin, transition metal compounds have, over the past decade, been shown to offer great versatility and chemical diversity not always seen in organic drugs.[5,19–23] Of the various promising antimalarial metal complexes of chloroquine, ferroquine, an organometallic analogue of chloroquine, has shown an enhanced activity in both the CQ-sensitive and CQ-resistant strains of *P. falciparum* compared to chloroquine.[1,5,24–26] Ferroquine is now undergoing phase IIb clinical trials, in which the efficacy of a combination of ferroquine and artefenomel[27] is being examined.[1,5,20,25,28,29] Other transition metal-based complexes which have subsequently shown promising antimalarial activity include those containing ruthenium,[30,31] rhodium[31,32] and iridium.[30–32]

Many of the metal-based antimalarial drug candidates synthesised to date share a common characteristic – they are all stoichiometric agents which react only once with their targets.[33] While many have shown success in this regard, this concept is limited by the often high doses of the metallodrug required to produce the desired effect, consequently resulting in significant toxicity and side-effects.[33] As an alternative strategy, the use of metallodrugs capable of performing catalytic reactions within biological systems is becoming increasingly popular.[34–36] In particular, great interest has been directed towards the use of metal-based catalytic compounds capable of interfering with the NAD^+/NADH transfer hydrogenation reactions within cancer cells as a novel mechanism of action.[37–39] While intracellular transfer hydrogenation reactions have been largely studied in terms of anticancer applications, in 2019, Stringer *et al.* tested two quinoline-based half-sandwich organoiridium and organorhodium complexes (Fig. 1) in the presence of sodium formate against the CQ-resistant K1 strain of *P. falciparum*.[40] Although only a preliminary study, it demonstrated that co-administration of metal-based complexes with a hydrogen source may be useful in targeting essential co-factors such as NAD^+, showing a stepwise decrease in parasite viability and thereby possibly overcoming resistance mechanisms within the parasite.

Herein we describe the synthesis and characterisation of neutral and cationic half-sandwich iridium(III) complexes containing 7-chloroquinoline-1,2,3-triazole ligands. These complexes have been evaluated against the chloroquine-sensitive (CQS) NF54 and the chloroquine-resistant (CQR) K1 strains of *P. falciparum*, as well as against the mammalian Chinese Hamster Ovarian cell line. This study also explores several possible mechanisms of action of these compounds, including a preliminary investigation into their transfer hydrogenation catalytic abilities.

Results and discussion

Synthesis and characterisation

The synthesis of the series of 7-chloroquinoline-1,2,3-triazole ligands (**2a–g**) required two synthetic steps, as outlined in Scheme 1. The first step involved the synthesis of 4-azido-7-chloroquinoline, **1**, from 4,7-dichloroquinoline and excess sodium azide following a reported literature procedure.[10]

The second step involved reacting 4-azido-7-chloroquinoline **1** with various aromatic alkynes *via* a "click" reaction following the methodology of Sharpless and co-workers[41,42] for the Cu(I)-catalysed azide–alkyne 1,3-dipolar cycloaddition (CuAAC) reaction. The different aromatic alkynes were chosen for the synthesis of ligands **2a–g** according to the electron-withdrawing or -donating effect of the respective side-group. In general, the synthesis of the ligands proceeded easily and quickly, resulting in white and pale-yellow solids in low to excellent yields of 23–83%. All seven ligands were characterized by ^{1}H NMR and $^{13}C\{^1H\}$ NMR spectroscopy, IR spectroscopy and liquid chromatography-mass spectrometry, with all having a purity greater than 95%.

The synthesis of the neutral cyclometallated iridium(III) pentamethylcyclopentadienyl 7-chloroquinolinotriazole complexes (**3a–e**) was achieved *via* sodium acetate-mediated C–H activation (Scheme 1). Surprisingly, the synthesis of the cyclometallated iridium(III) complexes did not follow the mild conditions prescribed for reactions of this kind,[43] instead, refluxing in acetonitrile at over 65 °C for almost a week was required. When this reaction was initially attempted at room temperature, a bright yellow precipitate formed which revealed that the metal had coordinated to the more basic quinoline nitrogen in a monodentate manner, as shown by complex **4** in Scheme 2. Upon heating the monodentate complexes in acetonitrile to a temperature of 65 °C and above, the bright yellow precipitate gradually dissolved and, when cooled, another yellow precipitate formed. This precipitate was that of the desired cyclometallated iridium(III) complexes, **3a–e**. Using computational analyses comprising dispersion-corrected DFT quantum chemical calculations, we briefly probed the hypothesis that kinetic (monodentate quinoline coordination) *versus* thermodynamic (cyclometallated) controlled rearrangement is taking place. The preliminary computational simulations are included in the ESI† and support the hypothesis that the complex **3a** is the

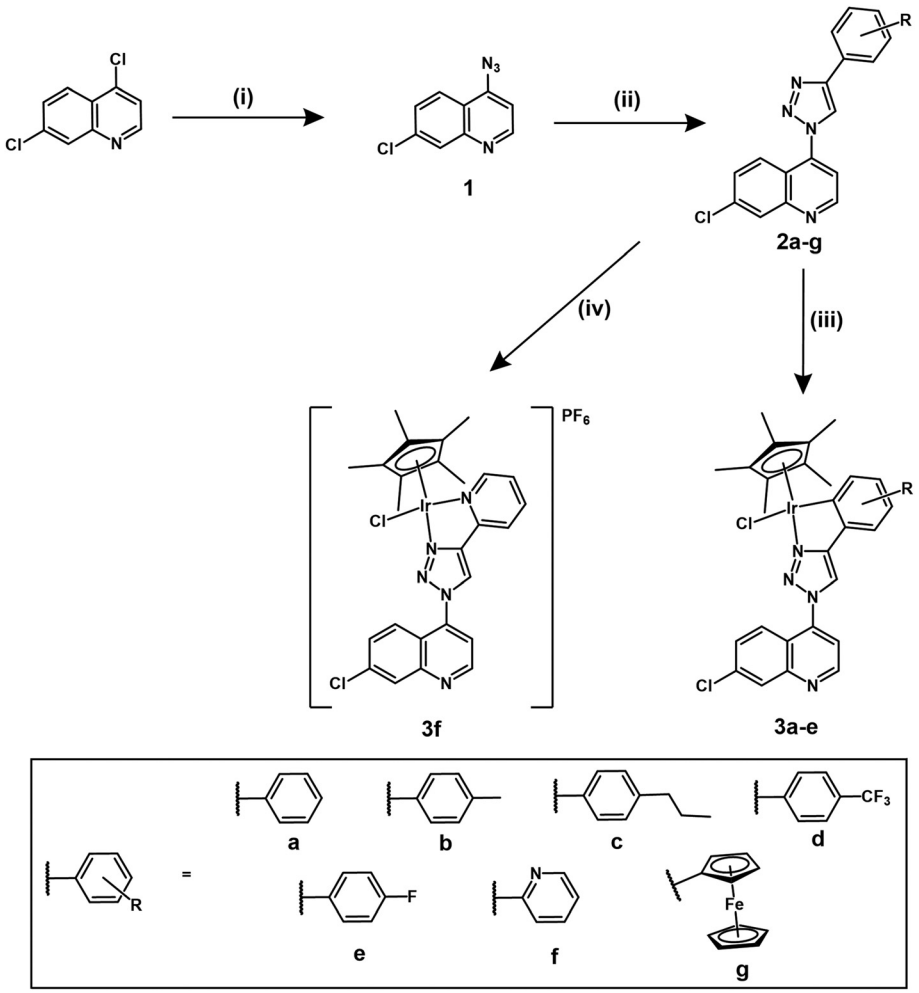

Scheme 1 Synthesis of 7-chloroquinoline-1,2,3-triazole ligands (**2a–g**) and their corresponding iridium(III) complexes (**3a–f**). Reagents and conditions: (i) NaN_3, DMF, 65 °C, 5 h; (ii) aromatic alkyne, *t*-BuOH or CH_2Cl_2/H_2O (1 : 1), $CuSO_4{\cdot}5H_2O$, sodium ascorbate, 30 °C, 2–72 h; (iii) $[IrCp^*(\mu\text{-}Cl)Cl]_2$ (0.7 eq.), NaOAc (2 eq.), CH_3CN, 65 °C (72 h), r.t. (72 h); (iv) $[IrCp^*(\mu\text{-}Cl)Cl]_2$ (0.5 eq.), NH_4PF_6 (4 eq.), CH_2Cl_2/EtOH, r.t., 22 h.

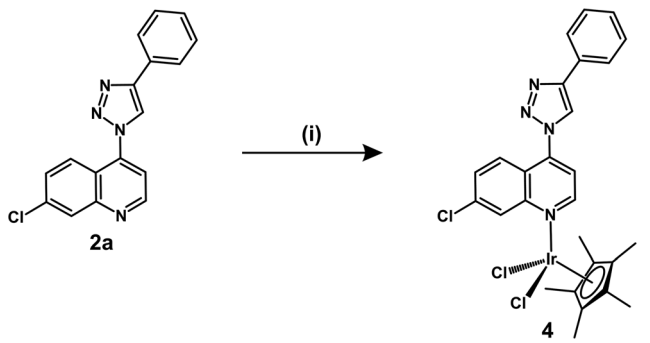

Scheme 2 Synthesis of the neutral monodentate iridium(III) 7-chloroquinolinotriazole complex, **4**. Reagents and conditions: (i) $[IrCp^*(\mu\text{-}Cl)Cl]_2$ (0.7 eq.), NaOAc (2 eq.), MeCN, r.t., ~1 min.

thermodynamic product while complex **4** is the kinetic product. The synthesis of the cationic *N*,*N*-chelated half-sandwich iridium(III) 7-chloroquinolinotriazole complex (**3f**) was achieved *via* a bridge-splitting reaction of the iridium dimer and coordination of the ligand **2f**, as shown in Scheme 1. A salt metathesis using hexafluorophosphate was used to replace the chloride counterion and to allow for the precipitation of the cationic complex **3f** in a good yield of 79%. The complexes were all characterised using ^1H NMR and $^{13}C\{^1H\}$ NMR spectroscopy, with a singlet at 1.81 ppm (**3a–e**) or 1.76 ppm (**3f**) integrating for 15 protons corresponding to the methyl protons on the Cp* ligand. Further evidence for the coordination of the ligands to the metal centre is the absence of a proton signal at the *ipso*-carbon of C–H activation for neutral complexes **3a–e** relative to the ^1H NMR spectra of their respective ligands. The most abundant peak in the ESI mass spectra of the complexes are generally associated with the loss of a chloride ligand.

Single crystal X-ray diffraction

Single crystals of the cyclometallated complex **3a** and the monodentate complex **4** were grown by the slow diffusion of diethyl ether into a concentrated dichloromethane solution and analysed using single crystal X-ray diffraction analysis.

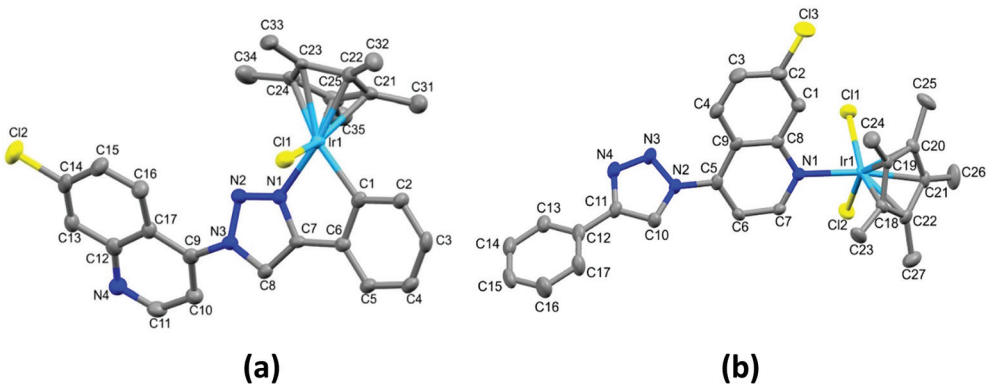

Fig. 2 Molecular structures of neutral iridium(III) Cp* 7-chloroquinolinotriazole complexes (a) **3a** (cyclometallate) and (b) **4** (monodentate), where thermal ellipsoids are drawn at 40% and 50% probability level, respectively. Hydrogen atoms have been omitted for clarity.

From the Mercury diagrams of complexes **3a** and **4** (Fig. 2), it can be seen that both iridium(III) complexes adopt a "three-legged piano-stool" structure. This piano-stool structure and the bond lengths and angles around the metal centre are commonly observed in many other analogous iridium, rhodium and ruthenium half-sandwich complexes.[31,44,45]

Table S1† summarises the crystal data and refinement parameters for both complexes. Complex **3a** crystallizes in the monoclinic $P2_1/c$ space group while complex **4** crystallises in the orthorhombic *Pbca* space group. Selected bond distances and angles for both complexes are listed in Table S2.† The bond distance between the metal centre and the chloride ligand for both complexes **3a** and **4** is approximately 2.4 Å, whereas the distance between the metal centre and the two chelating atoms of complex **3a** is 2.062 Å and 2.071 Å for C1 and N1, respectively (Fig. 2a). Similar distances are observed in the literature for cyclometallated iridium(III) complexes.[31] In the case of monodentate complex **4**, however, the bond distance between the metal centre and N1 (Fig. 2b) is longer at 2.159 Å, which is similar to that observed for another monodentate Ir(III) complex in the literature.[46] The data in Table S2† also suggests that the geometry around the metal centre is pseudo-tetrahedral as the bond angles around the metal centre range between 77.58 and 88.39° for both complexes. For complex **3a**, the new 5-membered ring formed by cyclometallation is not entirely planar as expected, with a torsion angle of 4.6°, while the quinoline moiety and the triazole-phenyl ring system of this complex are also not co-planar, with a torsion angle of 32.5°. In the case of the monodentate complex, **4**, the quinoline moiety and the triazole-phenyl ring system are similarly not co-planar, but rotated 47.8° from each other. Also, without the rigidity afforded by cyclometallation, the torsion angle between the triazole and phenyl rings is 22.8°, much larger than the corresponding angle of 4.6° for the cyclometallated complex.

In vitro antiplasmodial and cytotoxicity assays

The 7-chloroquinoline-1,2,3-triazole ligands (**2a–g**) and the iridium(III) half-sandwich complexes (**3a–f**, **4**) were evaluated *in vitro* for their antiplasmodial activity against the NF54 chloroquine-sensitive (CQS) strain of *P. falciparum*. The complexes that displayed good, micromolar activity were also tested for activity against the chloroquine-resistant (CQR) K1 strain. Furthermore, five of the most active metal complexes, namely **3a**, **3b** and **3d–f**, were tested for cytotoxicity against the mammalian Chinese Hamster Ovarian (CHO) cell line. Chloroquine diphosphate (CQDP) and emetine were used as the control drugs in this study. The biological results for the ligands and the iridium(III) complexes are summarised in Tables 1 and 2, respectively.

All ligands tested (*i.e.* **2a–g**) were found to display relatively poor antiplasmodial activity against the CQS NF54 strain of *P. falciparum*. The IC_{50} values for these ligands ranged from 9.87 μM (**2c**) to 28.02 μM (**2f**), with the ferrocenyl compound **2g** having an IC_{50} value of 12.30 μM, as listed in Table 1. The activity of the ligands is significantly enhanced upon metal complexation with iridium, with some complexes being over one hundred times more active than their respective ligands (Table 2). This suggests that the metal entity could play a role in reducing parasite viability, which may be linked to an increase to the overall lipophilicity of the compound or to the interaction of the metal centre with target compounds, although the mechanism for this is still unknown. The most active complex of all the Ir(III) complexes is the cationic *N*,*N*-chelated complex **3f**, with a submicromolar IC_{50} value of 0.25 μM. Of the neutral cyclometallated complexes, complex **3a** displayed the best activity (0.69 μM), followed by **3e** (0.99 μM) and **3b** (1.02 μM). This shows that introducing more

Table 1 *In vitro* antiplasmodial activity of 7-chloroquinoline-1,2,3-triazole ligands **2a–g** against the CQS (NF54) strain of *P. falciparum*

Compound	R-substituent	IC_{50} (μM) ± SE NF54
2a	H	22.73 ± 3.48
2b	CH_3	19.88 ± 3.46
2c	$(CH_2)_2CH_3$	9.87 ± 0.57
2d	CF_3	22.30 ± 4.43
2e	F	18.28 ± 0.65
2f	Pyridyl	28.02 ± 1.37
2g	Fc	12.30 ± 2.56
CQDP	—	0.01 ± 0.002

Table 2 *In vitro* antiplasmodial activity of iridium(III) half-sandwich complexes **3a–f** and **4** against the CQS (NF54) and CQR (K1) strains of *P. falciparum*. Activities for selected iridium(III) complexes against the Chinese Hamster Ovarian (CHO) cell line are also reported

Compound	R-substituent	IC_{50} (μM) ± SE NF54	IC_{50} (μM) ± SE K1	IC_{50} (μM) ± SE CHO	Resistance index (RI)[a]	Selectivity index (SI)[b]
3a	H	0.69 ± 0.17	1.06 ± 0.16	78.67 ± 3.07	1.54	114.01
4	H	48.45 ± 1.73	ND[c]	ND	ND	ND
3b	CH_3	1.02 ± 0.17	2.22 ± 0.18	25.64 ± 1.43	2.18	25.14
3c	$(CH_2)_2CH_3$	2.34 ± 0.38	3.06 ± 0.22	ND	1.31	ND
3d	CF_3	1.10 ± 0.16	2.59 ± 0.45	54.59 ± 4.16	2.35	49.63
3e	F	0.99 ± 0.22	1.01 ± 0.20	104.01 ± 16.8	1.02	105.06
3f	Pyridyl	0.25 ± 0.11	0.65 ± 0.06	123.54 ± 4.65	2.60	494.16
CQDP		0.01 ± 0.002	0.13 ± 0.04	ND	12.64	ND
Emetine		ND	ND	0.12 ± 0.04	ND	ND

[a] (IC_{50} K1/IC_{50} NF54). [b] (IC_{50} CHO/IC_{50} NF54). [c] ND = not determined.

hydrophobic side groups to metal complexes does not necessarily confer greater antiplasmodial activity, since the unsubstituted complex **3a** was the most active of the neutral series. The antiplasmodial activity of complex **4**, in which the ligand is coordinated in a monodentate fashion to the iridium *via* the quinoline nitrogen, was also determined. This complex was found to have poor activity, with an IC_{50} value of 48.4 μM, indicating that the stability conferred by metal coordination has a large impact on parasite viability.

The inhibitory data for these compounds tested against the K1 strain somewhat resembles the trend observed for the NF54 strain. The resistance indices (RI) were, in most cases, slightly greater than 1 with some even being greater than 2. These RI values suggest that the complexes likely experience mild cross-resistance similar to, albeit not to the same extent, as that of chloroquine (RI value = 12.6).

The results in Table 2 also show that all five of the compounds (**3a,b,d–f**) tested against the CHO cell-line are not cytotoxic compared to the control, emetine. The selectivity index (SI) values for the five tested complexes indicate that they have far greater selectivity towards the parasitic cells, with cationic complex **3f** being almost 500 times more selective towards the parasite than the mammalian cell line.

Speed-of-action studies

One of the ideal criteria for new drug candidates is that they are fast-acting, thereby providing a rapid relief of symptoms for the infected patient.[47,48] This is also to ensure that very few parasites survive after drug exposure, thereby lowering the occurrence of mutations that could lead to the development of new drug resistance mechanisms.[47,48]

In order to evaluate the speed of action of the synthesised iridium(III) complexes with the greatest antiplasmodial activity (**3a**, **3e** and **3f**), an assay experiment was performed following a modified method of the "IC_{50} speed assay" previously described by Le Manach *et al.*[49] A schematic representation of this assay is shown in Fig. 3. The assay was performed using synchronized ring cultures of the chloroquine-sensitive NF54 strain in order to determine whether compounds **3a**, **3e** and **3f** are either fast- or slow-acting. Known antimalarial agents, chloroquine (CQ), ferroquine (FQ) and artemisinin (ART) were used as the controls in this experiment.

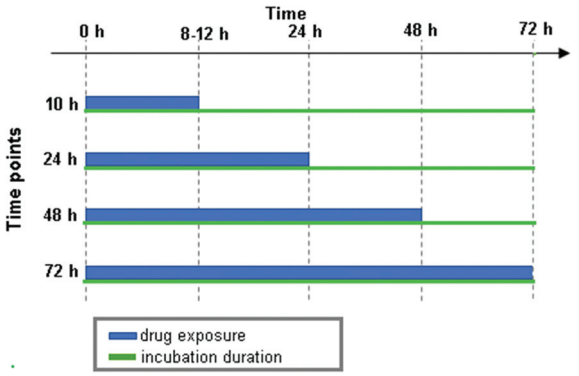

Fig. 3 Schematic representation of the *in vitro* speed-of-action assay.

The results of this speed of action experiment are summarised in Fig. 4. The IC_{50} values determined at the 10-, 24- and 48-hour time-points are represented as a ratio relative to the 72-hour time-point. The dotted line at a ratio of 1.0 therefore represents the baseline IC_{50} ratio at 72 hours (*i.e.* IC_{50} 72 h/IC_{50} 72 h = 1.0). Compounds which have an IC_{50} ratio (relative to 72 hours) of 1 or less than 1 early in the incubation period are described as "fast-acting" while those with ratios greater than 1 are described as "slow-acting". The respective IC_{50} 24 h/IC_{50} 72 h ratios of 0.9, 0.8 and 1.0 for the controls, CQ, ART

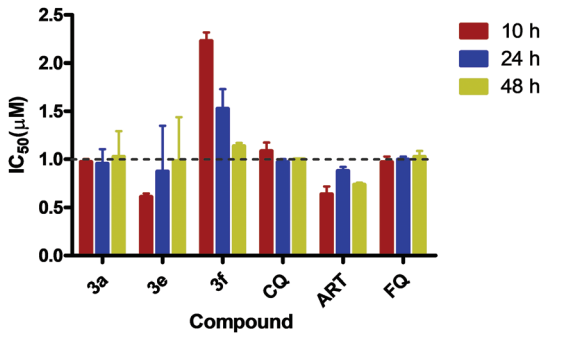

Fig. 4 IC_{50} speed assay profiles of **3a**, **3e**, and **3f**, as well as controls, CQ, ART and FQ. The mean IC_{50} values at each time point are presented as ratios relative to the IC_{50} value of the standard 72-hour assay. The dotted line indicates the baseline IC_{50} ratio at 72 hours.

and FQ, are indicative of these drugs being fast-acting compounds, which has been observed in previous experiments.[49] Similarly, compounds **3a** and **3e** also have their onset of action within 24 hours, with their respective IC_{50} 24 h/IC_{50} 72 h ratios being 0.9 and 0.8, respectively, meaning they are likely fast-acting compounds. In contrast to this, the IC_{50} ratio of **3f** at 10 hours is 2.3-fold higher than the respective IC_{50} value at the 72-hour time point. The IC_{50} 24 h/IC_{50} 72 h ratio only reaches 1.2 after 48 h of drug exposure; therefore, **3f** demonstrates the characteristics of a slow-acting compound.

β-Haematin inhibition studies

Like chloroquine, the target for many aminoquinoline-based compounds is the erythrocytic stage of the life cycle of *P. falciparum* and, more specifically, the formation of haemozoin.[1,3,5] The ability of a compound to inhibit haemozoin formation can be evaluated using the Nonidet P-40 (NP-40) detergent-mediated β-haematin inhibition assay, with β-haematin being the synthetic form of haemozoin.[50] The ferrocenyl ligand (**2g**), one neutral complex (**3d**) and the cationic complex (**3f**) were the representative compounds tested for their ability to inhibit β-haematin formation, the dose–response curves of which are shown in Fig. 5. The compounds were all screened in triplicate up to a concentration of 1 mM and the amount of synthetic haemozoin formed was quantified using the colorimetric pyridine ferrochrome method published by Egan *et al.*[51] All of the compounds tested were found to inhibit β-haematin formation, indicated by the characteristic sigmoidal curve for each, likely due to the presence of a quinoline scaffold in all their structures. Their activity, however, was lower than or comparable to chloroquine itself, which has an IC_{50} value of 65.3 μM. The neutral complex, **3d**, appeared to have the best β-haematin inhibitory activity (73.2 μM) while the ferrocenyl ligand, **2g**, has the worst (362.5 μM). Since the results of this cell-free assay suggest that these compounds do inhibit the formation of β-haematin, they may be likely candidates for the inhibition of haemozoin in the parasite.

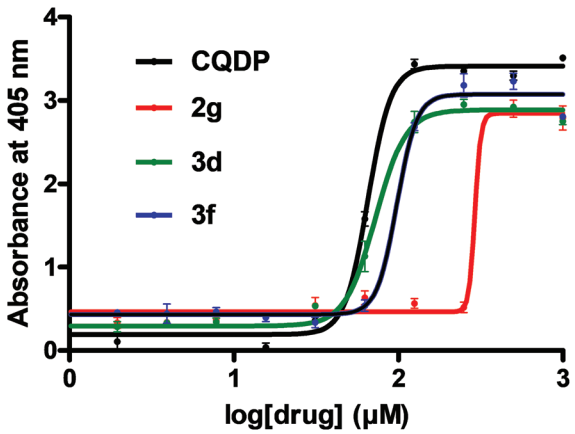

Fig. 5 Dose–response curves obtained for compounds **2g**, **3d** and **3f**, as well as CQDP, using the NP-40 detergent-mediated β-haematin inhibition assay.

Preliminary transfer hydrogenation studies

In recent years, it has been suggested that a disturbance in the intracellular NAD^+/NADH ratio may affect the cellular redox status, thereby bringing about metabolic changes and possibly even cell death.[38] It is for this reason that significant attention has been given to the use of organometallic complexes capable of the regioselective reduction of NAD^+ to 1,4-NADH under biological conditions.[52] The complexes that displayed the best antiplasmodial activity, namely **3a** and **3f**, were therefore tested for their ability to regioselectively catalyse the transfer hydrogenation reduction of NAD^+ to NADH, using sodium formate as the hydrogen source. To demonstrate this, qualitative tests by means of ^{1}H NMR spectroscopy were performed using complexes **3a** and **3f** as catalyst precursors. In the ^{1}H NMR experiment for complex **3a** (Fig. 6), the spectrum at t = 0 hours shows predominantly the presence of NAD^+, however, the presence of signals pertaining to 1,4-NADH are also observed at this time. This means that the catalytic reduction begins immediately once all the reactants are in solution. After 4 hours, the absence of characteristic NAD^+ signals indicated that no more NAD^+ was present in solution, with only signals characteristic of 1,4-NADH observed at this time interval. This indicates that neutral cyclometallated iridium(III) complex **3a** is capable of catalysing the regioselective reduction of NAD^+ to 1,4-NADH, using sodium formate as the hydrogen source. The cationic iridium(III) complex **3f**, which exhibited the best antiplasmodial activity of all the tested complexes, was also tested but did not exhibit effective catalytic ability in reducing NAD^+ to NADH (Fig. S28†).

In order to verify further the transfer hydrogenation catalytic ability of the iridium(III) 7-chloroquinoline-1,2,3-triazole complexes, a cell-free experiment, modified from the pLDH method (Fig. 7a), was used. This modified method was first described by Stringer *et al.* for detecting the cell-free catalytic ability of *N*,*O*-chelating quinoline-based half-sandwich rhodium and iridium complexes.[40] If the complexes can facilitate the reduction of NAD^+ to NADH in the presence of sodium formate, the NADH should reduce the added nitroblue tetrazolium (NBT) to formazan, as shown in Fig. 7a. The absorbance at 600 nm is then taken and is proportional to the amount of dark blue formazan present, therefore providing a means of detecting the transfer hydrogenation catalytic ability of the complexes. Following this method, different concentrations of neutral complexes **3a** and **3e** were incubated with NAD^+ and sodium formate at 37 °C and pH 7.4 for 6 hours. The results of this cell-free assay experiment are shown in Fig. 7b. Although this is an indirect method of detecting coenzyme conversion, the results show that complexes **3a** and **3e**, in the presence of sodium formate, can act as transfer hydrogenation catalysts, facilitating the reduction of NAD^+ to NADH in a cell-free environment. While complex **3e** displays slightly better catalytic activity than complex **3a**, both demonstrate a positive correlation between the concentration of the complex and the amount of formazan formed.

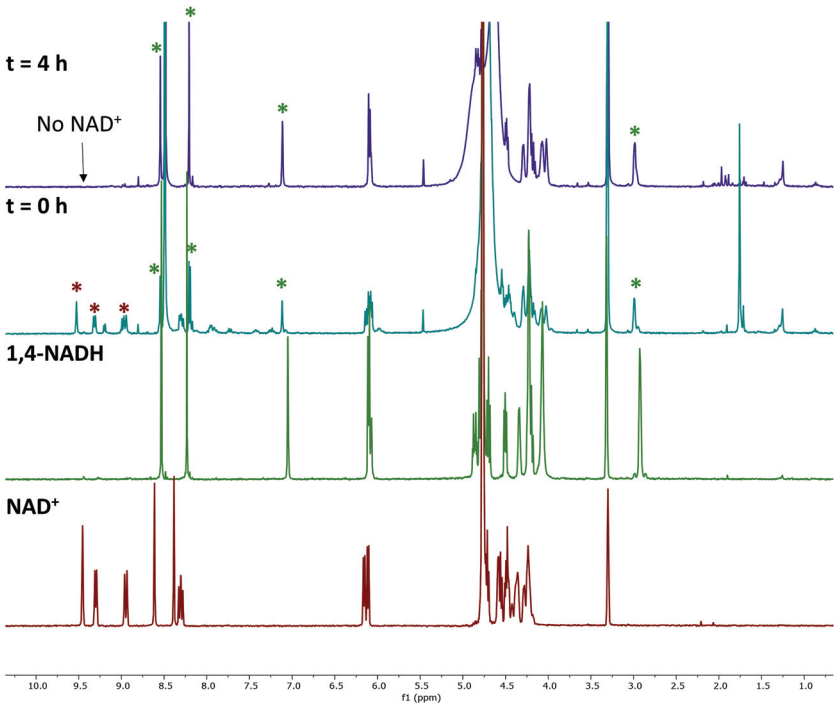

Fig. 6 ^{1}H NMR spectra of a mixture of iridium(III) complex **3a**, NAD^+ and sodium formate in $MeOD/D_2O$ at 37 °C. Signals marked by (*) represent NAD^+ and (*) represent 1,4-NADH.

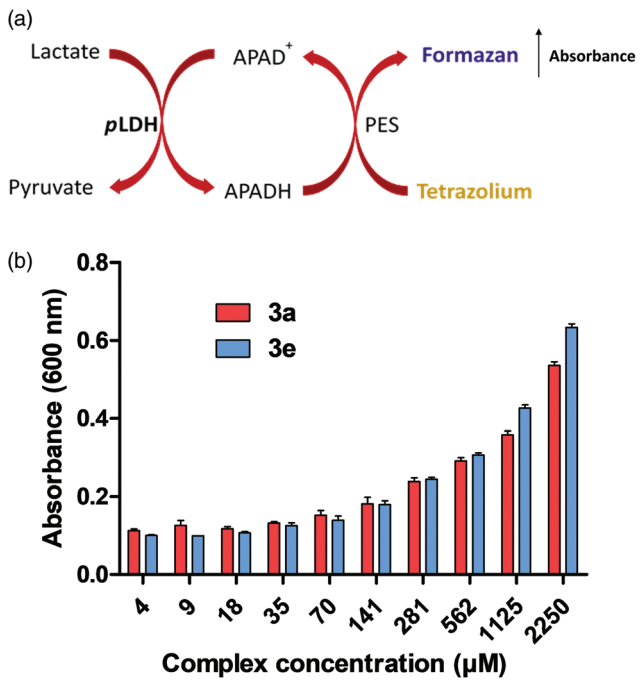

Fig. 7 (a) Principle of the pLDH Malstat™ assay for the detection of parasite viability; (b) absorbance values determined for increasing concentrations of the complexes **3a** and **3e**.

Conclusions

Various 7-chloroquinoline-1,2,3-triazole-based ligands (**2a–g**) were synthesised and the reaction of selected ligands with $[IrCl(\mu\text{-}Cl)(Cp^*)]_2$ yielded five neutral, cyclometallated iridium (III) complexes (**3a–e**) and one cationic, *N*,*N*-chelated iridium (III) complex (**3f**). The synthesis of the cyclometallated complexes revealed a surprising result – the ligands first coordinate to the metal in a monodentate fashion *via* the quinoline nitrogen before subsequent detachment and rearrangement to form the cyclometallated product. Computational analyses of the reaction of ligand **2a** with $[IrCl(\mu\text{-}Cl)(Cp^*)]_2$ support the hypothesis that complex **3a** is a thermodynamic product while complex **4** is a kinetic product. The structures and nature of metal-coordination of these complexes (**3a** and **4**) were confirmed using single-crystal X-ray diffraction. Upon coordination of ligands **2a–f** with iridium to form complexes **3a–f**, the antiplasmodial activity is significantly enhanced, with some complexes being over one hundred times more active than their respective ligands. The cationic complex **3f** displayed the best antiplasmodial activity while the monodentate complex **4** displayed very poor activity, indicating that the location of metal coordination is important. In general, the complexes showed decreased activity against the chloroquine-resistant (K1) strain compared to that in the chloroquine-sensitive (NF54) strain. Furthermore, selected active complexes (**3a, b,d–f**) tested against the mammalian Chinese Hamster Ovarian cell line were non-cytotoxic and were more selective towards the parasite than the healthy cells. An "IC_{50} speed assay" against the chloroquine-sensitive (NF54) strain found cyclometallated complexes **3a** and **3e** to be fast-acting compounds that reach their lowest IC_{50} values within 24 hours. Cationic complex **3f** was, however, found to be slow-acting, only reaching its lowest IC_{50} value after 48 hours. To gain

insight into a potential mechanism of action of these compounds, selected compounds (**2g**, **3d** and **3f**) were tested for their ability to inhibit the formation of β-haematin. All were found to inhibit the formation of β-haematin, some to a greater extent than others, but none to the extent of the control drug chloroquine. Finally, through preliminary ^{1}H NMR experiments and a cell-free assay adapted from the pLDH assay, it was found that neutral complexes **3a** and **3e** may be capable of acting as transfer hydrogenation catalysts, affecting regioselective reduction of NAD^{+} to NADH. Conversely, cationic complex **3f** is not an effective transfer hydrogenation catalyst as it showed no catalytic activity over 4 hours. It can therefore be assumed that this complex likely acts with a different mechanism of action which confers excellent antiplasmodial activity within the parasite.

Experimental

General details

All reagents and solvents were purchased from commercial sources (Sigma-Aldrich, Merck and KIMIX) and were used without further purification. Iridium(III) trichloride trihydrate was purchased from Heraeus SA. The iridium dimer, $[IrCp^{*}(\mu\text{-}Cl)Cl]_2$ and compounds **1**, **2a**, **2b** and **2e** were synthesised following literature methods.[10,53] All reactions were carried out under an inert argon atmosphere using standard Schlenk line techniques unless otherwise stated. Nuclear magnetic resonance (NMR) spectra were recorded on a Bruker XR600 MHz spectrometer (^{1}H at 599.95 MHz and $^{13}C\{^{1}H\}$ at 151.0 MHz), a Bruker Topspin GmbH (^{1}H at 400.22 MHz, $^{13}C\{^{1}H\}$ at 100.65 MHz, $^{19}F\{^{1}H\}$ at 376.58 MHz and $^{31}P\{^{1}H\}$ at 162.01 MHz) or a Varian Mercury 300 (^{1}H at 300.08 MHz) spectrometer. These were equipped with a Bruker Biospin GmbH casing and sample injector at 30 °C and tetramethylsilane (TMS) was used as the internal standard. Infrared (IR) spectroscopy was performed on a PerkinElmer Spectrum 100 FT-IR spectrometer using Attenuated Total Reflectance (ATR) with vibrations measured in units of cm^{-1}. Purity was determined using an analytical Agilent HPLC 1260 equipped with an Agilent infinity diode array detector (DAD) 1260 UV-Vis detector, with an absorption wavelength range of 210–640 nm. High resolution (HR) electrospray ionisation mass spectrometry (ESI-MS) was performed on a Waters Synapt G2 QTOF mass spectrometer with data recorded using the positive mode. Melting points were obtained using a Büchi Melting Point Apparatus B-540 and are uncorrected.

Synthesis

General procedure for the synthesis of ligands 2a–2g. 4-Azido-7-chloroquinoline (**1**) and a commercial alkyne were dissolved in either dichloromethane or *t*-BuOH (2.00 mL). A freshly prepared solution of sodium ascorbate (0.6 eq.) and $CuSO_4{\cdot}5H_2O$ (0.3 eq.) in water (2.00 mL) was then added to the reaction mixture. This was allowed to stir at 30 °C for 2–72 h and stopped when the reaction was completed, as shown by thin layer chromatography analysis. To the resulting reaction mixture, dichloromethane (30.0 mL) was added, which was then washed with a saturated NH_4Cl solution (3 × 30.0 mL) to remove Cu^{2+} ions and subsequently washed with water (3 × 30.0 mL). The solution was then dried using anhydrous Na_2SO_4, filtered and the solvent was thereafter removed from the filtrate. Purification was achieved *via* recrystallization from hot MeOH to yield the pure desired solid product.

7-Chloro-4-(4-(4-propylphenyl)-1*H*-1,2,3-triazol-1-yl)quinoline (2c). To a solution of **1** (0.200 g, 0.977 mmol) and 1-eth-1-ynyl-4-propylbenzene (0.155 mL, 0.977 mmol) in dichloromethane (2.00 mL), a solution of sodium ascorbate and $CuSO_2{\cdot}5H_2O$ in water (2.00 mL) was added and the reaction mixture was left to stir for 19 h at 30 °C. **Yield:** 0.0805 g, (23.4%). **^{1}H NMR (400 MHz, $CDCl_3$):** δ (ppm) = 9.09 (1H, br d, J = 5.71 Hz, H-2); 8.26 (1H, d, J = 1.90 Hz, H-8); 8.20 (1H, s, H-11); 8.08 (1H, d, J = 9.08 Hz, H-5); 7.86 (2H, d, J = 8.21 Hz, H-14); 7.61 (1H, dd, J = 1.98, 9.09 Hz, H-6); 7.56 (1H, d, J = 4.51 Hz, H-3); 7.31 (2H, d, J = 8.24 Hz, H-15); 2.66 (2H, t, H-17); 1.76–1.64 (2H, m, H-18); 0.98 (3H, t, H-19); **$^{13}C\{^{1}H\}$ NMR (101 MHz, $CDCl_3$):** δ (ppm) = 151.55 (C-2), 150.65 (C-9), 148.94 (C-12), 143.88 (C-7), 141.18 (C-13), 137.09 (C-4), 129.61 (C-6), 129.35 (C-8, 15), 127.12 (C-16), 126.09 (C-14), 124.90 (C-5), 120.93 (C-10), 120.85 (C-11), 116.56 (C-3), 38.02 (C-17), 24.56 (C-18), 13.91 (C-19). **IR (ATR):** (ν_{max}/cm^{-1}) 2961, 2930, 2859, 1609, 1595, 1559 (Ar C=N). **Melting point:** 138.5–139.5 °C. **Purity:** 99.3% by LC (t_R 2.78 min).

7-Chloro-4-(4-(4-(trifluoromethyl)phenyl)-1*H*-1,2,3-triazol-1-yl)quinoline (2d). To a solution of **1** (0.200 g, 0.977 mmol) and 1-ethynyl-4-(trifluoromethyl)benzene (0.206 mL, 1.46 mmol) in dichloromethane (2.00 mL), a solution of sodium ascorbate and $CuSO_2{\cdot}5H_2O$ in water (2.00 mL) was added and the reaction mixture was left to stir for 20 h at 30 °C. **Yield:** 0.235 g (64.2%). **^{1}H NMR (400 MHz, $CDCl_3$):** δ (ppm) = 9.09 (1H, d, J = 4.10 Hz, H-2); 8.32 (1H, s, H-11); 8.27 (1H, d, J = 1.98 Hz, H-8); 8.07 (2H, d, J = 8.05 Hz, H-14); 8.03 (1H, d, J = 9.08 Hz, H-5); 7.75 (2H, d, J = 8.19 Hz, H-15); 7.62 (1H, dd, J = 2.02, 9.08 Hz, H-6); 7.56 (1H, d, J = 4.60 Hz, H-3). **$^{13}C\{^{1}H\}$ NMR (101 MHz, $CDCl_3$):** δ (ppm) = 151.54 (C-2), 150.49 (C-9), 147.36 (C-12), 140.95 (C-7), 137.29 (C-13), 133.20 (C-4), 131.00 (q, $^{2}J_{C-F}$ = 32.7 Hz, C-16), 129.80 (C-6), 129.31 (C-8), 126.36 (C-14), 126.11 (br q, $^{3}J_{C-F}$ = 3.6 Hz, C-15), 124.60 (C-5), 124.33 (q, $^{1}J_{C-F}$ = 272.1 Hz, C-17), 122.10 (C-11), 116.18 (C-3). **$^{19}F\{^{1}H\}$ NMR (377 MHz, $CDCl_3$):** δ (ppm) = −62.73 (s). **IR (ATR):** (ν_{max}/cm^{-1}) 1623, 1610, 1592, 1560 (Ar C=N), 1324 (C–F stretch). **Melting point:** 181.3–182.7 °C. **Purity:** 99.2% by LC (t_R 2.72 min).

7-Chloro-4-(4-(pyridin-2-yl)-1*H*-1,2,3-triazol-1-yl)quinoline (2f). To a solution of **1** (0.200 g, 0.977 mmol) and 2-ethynylpyridine (0.109 mL, 1.08 mmol) in *t*-BuOH (2.00 mL), a solution of sodium ascorbate and $CuSO_2{\cdot}5H_2O$ in water (2.00 mL) was added and the reaction mixture was left to stir for 3 d at 45 °C. **Yield:** 0.128 g (42.5%). **^{1}H NMR (400 MHz, DMSO-d_6):** δ (ppm) = 9.29 (1H, s, H-11); 9.18 (1H, d, J = 4.66 Hz, H-2); 8.69–8.67 (1H, m, H-17); 8.30 (1H, d, J = 2.06 Hz, H-8); 8.19 (1H, dt, J = 1.08, 1.08, 7.91 Hz, H-14); 8.09 (1H, d, J = 9.11 Hz, H-5); 8.00 (1H, td, J = 1.81, 7.83, 7.87 Hz, H-15); 7.96 (1H, d, J = 4.62 Hz,

H-3); 7.80 (1H, dd, J = 2.20, 9.10 Hz, H-6); 7.44 (1H, ddd, J = 1.19, 4.82, 7.57 Hz, H-16). **^{13}C{^{1}H} NMR (101 MHz, DMSO-d_6):** δ (ppm) = 152.28 (C-2), 149.73 (C-17), 149.34 (C-13), 149.12 (C-10), 147.86 (C-12), 140.33 (C-8), 137.34 (C-15), 135.33 (C-4), 128.94 (C-7), 128.03 (C-9), 125.48 (C-6), 125.34 (C-11), 123.47 (C-16), 120.36 (C-5), 119.95 (C-14), 117.19 (C-3). **IR (ATR):** (ν_{max}/cm^{-1}) 1606 (C=N)$_{pyridyl}$, 1567 (C=N)$_{quinoline}$. **Melting point:** 153.8–155.1 °C. **Purity:** 98.7% by **LC** (t_R 2.51 min).

7-Chloro-4-(4-(ferrocenyl)-1*H*-1,2,3-triazol-1-yl)quinoline (2g). To a solution of **1** (0.100 g, 0.489 mmol) and ethynylferrocene (0.103 g, 0.489 mmol) in dichloromethane (2.00 mL), a solution of sodium ascorbate and $CuSO_4 \cdot 5H_2O$ in water (2.00 mL) was added and the reaction mixture was left to stir for 20 h at 30 °C. **Yield:** 0.142 g (70.2%). **^{1}H NMR (400 MHz, CDCl$_3$):** δ (ppm) = 9.07 (1H, d, J = 2.04 Hz, H-2); 8.25 (1H, d, J = 1.51 Hz, H-8); 8.09 (1H, d, J = 9.00 Hz, H-5); 7.89 (1H, s, H-11); 7.62 (1H, dd, J = 1.40, 8.92 Hz, H-6); 7.53 (1H, d, J = 2.81 Hz, H-3); 4.83 (2H, br s, H-14); 4.40 (2H, br s, H-15); 4.16 (5H, s, H-16). **^{13}C{^{1}H} NMR (101 MHz, CDCl$_3$):** δ (ppm) = 151.57 (C-2), 150.51 (C-9), 148.26 (C-12), 141.12 (C-7), 137.06 (d, C-4, C-13), 129.57 (C-6), 128.96 (C-8), 124.79 (C-5), 120.60 (C-10), 120.16 (C-11), 115.70 (C-3), 71.45–70.98 (m, C-16), 70.61–70.20 (m, C-15), 68.26–67.92 (m, C-14). **IR (ATR):** (ν_{max}/cm^{-1}) 1611, 1591, 1558 (Ar C=N). **Melting point:** 203.0–204.6 °C. **MS** (HR-ESI, m/z): 414.0333 (60%, [M]$^+$), calculated 414.0335.

General procedure for the synthesis of cyclometallated Ir(III) half-sandwich complexes (3a–3e). A solution of the desired ligand (1 eq.), [IrCp*(μ-Cl)Cl]$_2$ (0.7 eq.) and NaOAc (2 eq.) was made in anhydrous CH_3CN (20.0 mL). The reaction mixture was refluxed under argon at 65–75 °C for 48–72 h and then left to stir at room temperature for a further 72 h, after which a yellow precipitate formed. This precipitate was filtered and washed with CH_3CN. The resulting yellow powder was dissolved in dichloromethane and filtered through Celite™ to remove any excess NaOAc. The solvent was then reduced and Et_2O was added to produce a yellow precipitate, which was then filtered and dried.

Ir(III) triazole-phenyl complex (3a). A solution of **2a** (0.100 g, 0.326 mmol), [IrCp*(μ-Cl)Cl]$_2$ (0.182 g, 0.229 mmol) and NaOAc (0.0535 g, 0.652 mmol) was made in anhydrous CH_3CN (20.0 mL) and refluxed under nitrogen for 72 h. **Yield:** 0.128 g (58.9%). **^{1}H NMR (400 MHz, CDCl$_3$):** δ (ppm) = 9.06 (1H, d, J = 4.62 Hz, H-2); 8.27 (1H, d, J = 1.80 Hz, H-8); 8.14–8.16 (2H, m, H-5, 11); 7.79 (1H, d, J = 7.55, H-14); 7.65 (1H, dd, J = 1.97, 9.11 Hz, H-6); 7.50 (1H, d, J = 4.63 Hz, H-3); 7.44 (1H, d, J = 7.42 Hz, H-17); 7.06 (1H, t, J = 7.24 Hz, H-15); 6.88 (1H, t, J = 7.33 Hz, H-16); 1.81 (15H, s, H-20). **^{13}C{^{1}H} NMR (101 MHz, CDCl$_3$):** 159.74 (C-12), 158.61 (C-18), 151.70 (C-2), 150.44 (C-9), 140.59 (C-7), 137.13 (C-4), 136.23 (C-14), 134.75 (C-13), 129.74 (br s, 2C, C-6, 15), 129.29 (C-8), 124.77 (C-5), 122.72 (C-16), 122.27 (C-17), 120.28 (C-10), 118.66 (C-11), 116.02 (C-3), 89.00 (C-19), 9.25 (C-20). **IR (ATR):** (ν_{max}/cm^{-1}) 1611, 1586, 1560 (Ar C=N). **Melting point:** >280 °C dec. **MS** (HR-ESI, m/z): 633.1409 (100%, [M − Cl]$^+$), calculated 633.1397.

Ir(III) triazole-*p*-tolyl complex (3b). A solution of **2b** (0.0700 g, 0.218 mmol), [IrCp*(μ-Cl)Cl]$_2$ (0.122 g, 0.153 mmol) and NaOAc (0.0358 g, 0.436 mmol) was made in anhydrous CH_3CN (20.0 mL) and refluxed under nitrogen for 48 h. **Yield:** 0.0481 g, (32.3%).**^{1}H NMR (400 MHz, CDCl$_3$):** δ (ppm) = 9.05 (1H, d, J = 4.64 Hz, H-2); 8.27 (1H, d, J = 1.74 Hz, H-8); 8.18 (1H, d, J = 9.12 Hz, H-5); 8.10 (1H, s, H-11); 7.65 (1H, dd, J = 2.05, 9.11 Hz, H-6); 7.60 (1H, s, H-18); 7.50 (1H, d, J = 4.65 Hz, H-3); 7.34 (1H, d, J = 7.58 Hz, H-14); 6.69 (1H, d, J = 7.45 Hz, H-15); 2.30 (3H, s, H-17); 1.81 (15H, s, H-21). **^{13}C{^{1}H} NMR (101 MHz, CDCl$_3$):** 159.68 (C-12), 158.64 (C-19), 151.67 (C-2), 150.46 (C-9), 140.65 (C-16), 139.29 (C-7), 137.11 (C-4), 136.98 (C-18), 132.01 (C-13), 129.70 (C-6), 129.27 (C-8), 124.88 (C-5), 123.74 (C-15), 121.98 (C-14), 120.27 (C-10), 118.12 (C-11), 115.92 (C-3), 88.89 (C-20), 21.92 (C-17), 9.25 (C-21); **IR (ATR):** (ν_{max}/cm^{-1}) 1609, 1591, 1560 (Ar C=N). **Melting point:** 290 °C dec. **MS** (HR-ESI, m/z): 647.1555 (100%, [M − Cl]$^+$), calculated 647.1554.

Ir(III) triazole-propylphenyl complex (3c). A solution of **2c** (0.0510 g, 0.146 mmol), [IrCp*(μ-Cl)Cl]$_2$ (0.0815 g, 0.102 mmol) and NaOAc (0.0359 g, 0.438 mmol) was made in anhydrous CH_3CN (10.0 mL) and refluxed under argon for 72 h. **Yield:** 0.0618 g (85.2%). **^{1}H NMR (400 MHz, CDCl$_3$):** δ (ppm) = 9.05 (1H, d, J = 4.64 Hz, H-2); 8.27 (1H, d, J = 1.74 Hz, H-8); 8.18 (1H, d, J = 9.12 Hz, H-5); 8.10 (1H, s, H-11); 7.65 (1H, dd, J = 2.05, 9.11 Hz, H-6); 7.60 (1H, s, H-20); 7.50 (1H, d, J = 4.65 Hz, H-3); 7.34 (1H, d, J = 7.58 Hz, H-14); 6.69 (1H, d, J = 7.45 Hz, H-15); 2.68–2.49 (2H, m, H-17); 1.81 (15H, s, H-23); 1.75–1.63 (2H, m, H-18); 0.98 (3H, t, J = 7.26, 7.26 Hz, H-19). **^{13}C{^{1}H} NMR (101 MHz, CDCl$_3$):** 159.59 (C-12), 158.69 (C-21), 151.66 (C-2), 150.42 (C-9), 143.98 (C-16), 140.68 (C-7), 137.12 (C-4), 136.45 (C-20), 132.24 (C-13), 129.71 (C-6), 129.24 (C-8), 124.88 (C-5), 123.17 (C-15), 122.00 (C-14), 120.31 (C-10), 118.16 (C-11), 115.96 (C-3), 88.90 (C-22), 38.56 (C-17), 24.81 (C-18), 14.17 (C-19), 9.23 (C-23). **IR (ATR):** (ν_{max}/cm^{-1}) 2869, 2925, 2954, 1607, 1594, 1561 (Ar C=N). **Melting point:** 283 °C dec. **MS** (HR-ESI, m/z): 753.1960 (100%, [M − Cl + DMSO]$^+$), calculated 753.2005.

Ir(III) triazole-4-(trifluoromethyl)phenyl complex (3d). A solution of **2d** (0.050 g, 0.133 mmol), [IrCp*(μ-Cl)Cl]$_2$ (0.0744 g, 0.0934 mmol) and NaOAc (0.0328 g, 0.400 mmol) was made in anhydrous CH_3CN (10.0 mL) and refluxed at 75 °C under argon for 72 h. **Yield:** 0.0121 g (12.3%). **^{1}H NMR (400 MHz, CDCl$_3$):** δ (ppm) = 9.09 (1H, d, J = 4.65 Hz, H-2), 8.29 (1H, d, J = 2.02 Hz, H-8), 8.22 (1H, s, H-11), 8.05 (1H, d, J = 9.30 Hz, H-5), 8.04 (1H, s, H-18), 7.66 (1H, dd, J = 2.09, 9.11 Hz, H-6), 7.51–7.58 (2H, m, H-3, 14), 7.20 (1H, dd, J = 0.90, 7.91 Hz, H-15), 1.81 (15H, s, H-21); **^{13}C{^{1}H} NMR (101 MHz, CDCl$_3$):** 160.21 (C-12), 157.68 (C-19), 151.57 (C-2), 150.57 (C-9), 140.61 (C-13), 138.27 (C-7), 137.48 (C-4), 132.60 (br q, $^3J_{C-F}$ = 3.45 Hz, C-18), 130.62 (q, $^2J_{C-F}$ = 30.75 Hz, C-16), 130.10 (C-6), 129.49 (C-8), 124.68 (q, $^1J_{C-F}$ = 273.14 Hz, C-17), 124.33 (C-5), 122.00 (C-11), 120.41 (C-10), 119.79 (br q, $^3J_{C-F}$ = 3.58 Hz, C-15), 119.63 (C-14), 116.21 (C-3), 89.45 (C-20), 9.20 (C-21). **^{19}F{^{1}H} NMR (377 MHz, CDCl$_3$):** δ (ppm) = −62.13 (s). **IR (ATR):** (ν_{max}/cm^{-1}) 1618, 1606, 1595, 1560 (Ar C=N), 1314 (C–F stretch). **Melting point:** 280 °C dec. **MS** (HR-ESI, m/z): 779.1396 (100%, [M − Cl + DMSO]$^+$), calculated 779.1410.

Ir(III) triazole-4-fluorophenyl complex (3e). A solution of **2e** (0.0762 g, 0.235 mmol), $[IrCp^*(\mu\text{-}Cl)Cl]_2$ (0.131 g, 0.164 mmol) and NaOAc (0.0578 g, 0.704 mmol) was made in anhydrous CH_3CN (15.0 mL) and refluxed at 65 °C under argon for 72 h. **Yield:** 0.0336 g (29.8%). **^{1}H NMR (400 MHz, $CDCl_3$):** δ (ppm) = 9.08 (1H, d, J = 4.65 Hz, H-2), 8.28 (1H, d, J = 2.07 Hz, H-8), 8.10 (1H, d, J = 9.30 Hz, H-5), 8.09 (1H, s, H-11), 7.65 (1H, dd, J = 2.12, 9.12 Hz, H-6), 7.52 (1H, d, J = 4.65 Hz, H-3), 7.52–7.43 (2H, m, H-14, 17), 6.63 (1H, td, J = 2.36, 8.64, 8.80 Hz, H-15), 1.81 (15H, s, H-20). **^{13}C{^{1}H} NMR (101 MHz, $CDCl_3$):** 163.15 (d, $^1J_{C-F}$ = 251.43 Hz, C-16), 162.86 (d, $^3J_{C-F}$ = 4.89 Hz, C-18), 157.81 (C-12), 151.63 (C-2), 150.56 (C-9), 140.60 (C-7), 137.27 (C-13), 130.98 (C-4), 129.86 (C-6), 129.43 (C-8), 124.61 (C-5), 123.49 (d, $^3J_{C-F}$ = 8.68 Hz, C-14), 122.36 (d, $^2J_{C-F}$ = 17.83 Hz, C-17), 120.31 (C-10), 118.34 (C-11), 116.01 (C-3), 109.77 (d, $^2J_{C-F}$ = 23.34 Hz, C-15), 89.22 (C-19), 9.20 (C-20). **^{19}F{^{1}H} NMR (377 MHz, $CDCl_3$):** δ (ppm) = −112.15 (s). **IR (ATR):** (ν_{max}/cm^{-1}) 1615, 1590, 1560 (Ar C═N). **Melting point:** 283 °C dec. **MS** (HR-ESI, m/z): 729.1418 (100%, $[M - Cl + DMSO]^+$), calculated 729.1442.

Synthesis of neutral Ir(III) monodentate triazole-phenyl complex (4). A solution of ligand **2a** (0.0500 g, 0.163 mmol) and $[IrCp^*(\mu\text{-}Cl)Cl]_2$ (0.0649 g, 0.0815 mmol) was made in anhydrous CH_3CN (10.0 mL). The reaction mixture was stirred at room temperature under argon for 16 h. A bright yellow precipitate formed, which was then filtered and washed with CH_3CN, yielding complex **4** as a bright yellow powder. **Yield:** 0.0776 g (67.5%). **^{1}H NMR (300 MHz, $CDCl_3$):** δ (ppm) = 9.50 (1H, br s, H-2); 8.78 (1H, br s, H-8); 8.26 (1H, s, H-11); 8.13 (1H, d, J = 9.09 Hz, H-5); 7.98–7.95 (2H, m, H-14); 7.63 (1H, dd, J = 1.89, 9.11 Hz, H-6); 7.57 (1H, d, J = 5.13 Hz, H-3); 7.53–7.48 (2H, m, H-15); 7.45–7.40 (1H, m, H-16); 1.58 (15H, s, H-18). **^{13}C{^{1}H} NMR (101 MHz, $CDCl_3$):** δ (ppm) = 154.48 (C-2), 149.67 (C-9), 148.77 (C-12), 141.85 (C-7), 137.63 (C-4), 130.15 (C-8), 129.84 (C-6), 129.39 (C-13), 129.09 (C-15), 128.99 (C-16), 126.11 (C-14), 125.15 (C-5), 121.34 (C-11), 116.30 (C-3), 86.40 (C-17), 9.11 (C-18). **IR (ATR):** (ν_{max}/cm^{-1}) 1611, 1560 (C═N)$_{quinoline}$. **Melting point:** 235 °C dec with melt.

Synthesis of cationic Ir(III) *N,N*-chelated 7-chloroquinoline-triazole complex (3f). To a solution of **2g** (0.0300 g, 0.0975 mmol) in dichloromethane/EtOH (1 : 1, 10 mL), a solution of $[IrCp^*(\mu\text{-}Cl)Cl]_2$ (0.0388 g, 0.0487 mmol) in dichloromethane/EtOH (1 : 1, 10 mL) was added dropwise and the reaction mixture was left to stir at room temperature for 20 h. Thin layer chromatography confirmed that there was no ligand left in the mixture. The resulting mixture was filtered through Celite™ and washed with minimal dichloromethane/EtOH mixture. NH_4PF_6 (0.0640 g, 0.390 mmol) was added to the solution, which was allowed to stir at room temperature under argon for 90 min. The solvent was, thereafter, reduced to approximately 5.00 mL, cooled rapidly in an ice bath and then put into the fridge for 2 h. The precipitate was filtered, washed with cold EtOH and dried, yielding **3f** as a pale yellow solid. **Yield:** 0.0627 g (78.9%). **^{1}H NMR (400 MHz, DMSO-d_6):** δ (ppm) = 9.99 (1H, s, H-11), 9.31 (1H, d, J = 4.64 Hz, H-2), 9.03 (1H, d, J = 5.47 Hz, H-17), 8.45 (1H, d, J = 7.80 Hz, H-14), 8.41 (1H, d, J = 2.08 Hz, H-8), 8.34–8.40 (1H, m, H-15), 8.14 (1H, d, J = 4.64 Hz, H-3), 8.02 (1H, d, J = 9.04 Hz, H-5), 7.93 (1H, dd, J = 2.13, 9.10 Hz, H-6), 7.82 (1H, ddd, J = 1.52, 5.73, 7.42 Hz, H-16), 1.76 (15H, s, H-19); **^{13}C{^{1}H} NMR (101 MHz, DMSO-d_6):** 152.47 (C-2), 152.36 (C-17), 149.35 (C-9), 148.22 (C-13), 147.51 (C-12), 140.81 (C-15), 139.44 (C-7), 135.91 (C-4), 129.59 (C-6), 128.47 (C-11), 128.41 (C-8), 127.76 (C-16), 124.37 (C-5), 122.53 (C-14), 119.89 (C-10), 118.08 (C-3), 89.26 (C-18), 8.34 (C-19).**^{19}F{^{1}H} NMR (377 MHz, DMSO-d_6):** δ (ppm) = −70.19 (d, $^1J_{P-F}$ = −711.15 Hz). **^{31}P{^{1}H} NMR (162 MHz, DMSO-d_6):** δ (ppm) = −144.17 (sept., $^1J_{F-P}$ = −711.19 Hz). **IR (ATR):** (ν_{max}/cm^{-1}) 3470, 3145, 1630, 1614, 1594 (Ar C═N), 825 (P–F stretch). **Melting point:** 249.5–251.2 °C dec. **MS** (HR-ESI, m/z): 670.1107 (100%, $[M - PF_6]^+$), calculated 670.1116.

X-ray crystallography

Suitable single crystals of complexes **3a** and **4** were grown from the slow diffusion of diethyl ether into a concentrated dichloromethane solution. Single-crystal X-ray diffraction data were collected on a Bruker KAPPA APEX II DUO diffractometer using graphite-monochromated Mo-Kα radiation (λ = 0.71073 Å). Data collection was carried out at 173(2) K. The temperature was controlled by an Oxford Cryostream cooling system (Oxford Cryostat). Cell refinement and data reduction were performed using the program SAINT.[54] The data were scaled and absorption correction performed using SADABS.[55] The structure was solved by direct methods using SHELXS-97[55] and refined by full-matrix least-squares methods based on F^2 using SHELXL-2018[55] and using the graphics interface program X-Seed.[56,57] The programs X-Seed and POV-Ray were used to prepare molecular graphic images. All non-hydrogen atoms were refined anisotropically. All hydrogen atoms were placed in idealised positions and refined in riding models with U_{iso} assigned 1.2 or 1.5 times U_{eq} of their parent atoms and the bond distances were constrained to 0.95 and 0.98 Å.

Biological methods

***In vitro* antiplasmodial assay.** The test samples were tested in triplicate on one or two separate occasions against the chloroquine-sensitive (NF54) and chloroquine-resistant (K1) strains of *P. falciparum.* Continuous *in vitro* cultures of asexual erythrocyte stages of *P. falciparum* were maintained using a modified method of Trager and Jensen.[58] Quantitative assessment of antiplasmodial activity *in vitro* was determined *via* the parasite lactate dehydrogenase assay using a modified method described by Makler.[59] The test samples were prepared to a 20 mg mL^{-1} or a 2 mg mL^{-1} stock solution in 100% DMSO. Stock solutions were stored at −20 °C. Further dilutions were prepared on the day of the experiment. Chloroquine (CQ) was used as the reference drug in all experiments. A full dose–response was performed for all compounds to determine the concentration inhibiting 50% of parasite growth (IC_{50} value). Test samples were tested at a starting concentration of 10 μg mL^{-1} or 100 μg mL^{-1}, which was then serially diluted 2-fold in complete medium to give 10 concentrations, with the lowest concentration being 0.02 μg mL^{-1} or 0.2 μg mL^{-1} respectively.

The same dilution technique was used for all samples. The IC_{50} values were obtained using a non-linear dose response curve fitting analysis *via* Graph Pad Prism v.5.0 software.

***In vitro* cytotoxicity assay.** Compounds were tested for *in vitro* cytotoxicity against the mammalian, Chinese Hamster Ovarian (CHO) cell-line using the MTT (3-(4,5-dimethylthiazol-2-yl)-2,5-diphenyltetrazoliumbromide) assay. The MTT assay is used as a colorimetric assay for cellular growth and survival and compares well with other available assays. The CHO cell line was cultured in sterile flasks containing 10% foetal calf serum, 45% DMEM and 45% HAMS F-12 medium in an environment of 5% CO_2 at 37 °C. The cell monolayers were detached with trypsin then resuspended with 5 mL culture medium. The number of cells were counted with crystal violet dye on a counting chamber to achieve a concentration of 10^5 cells per mL. Cells were distributed in flat-bottomed 96-well plates and incubated at 37 °C for 24 h for attachment. The test samples were tested in triplicate on one occasion. The test samples were prepared to a 2 mg mL^{-1} stock solution in 10% MeOH or 10% DMSO and were tested as a suspension if not completely dissolved. Test compounds were stored at −20 °C until use. Emetine was used as the reference drug in all experiments. The initial concentration of emetine was 100 μg mL^{-1}, which was serially diluted in complete medium with 10-fold dilutions to give 6 concentrations, the lowest being 0.001 μg mL^{-1}. The same dilution technique was applied to all the test samples. The highest concentration of solvent to which the cells were exposed had no measurable effect on cell viability. After 48 h, an aliquot of 25 μL MTT was added to each well and plates were incubated at 37 °C for 4 h. Dimethyl sulfoxide (DMSO) was used to dissolve the MTT crystals. The plates were read at 570 nm with a Modulus™ microplate fluorometer. The IC_{50} values were obtained from plotting non-linear dose–response curves using Graph Pad Prism v.5.0 software.

***In vitro* speed of action assay.** A modified IC_{50} speed assay was followed in order to categorize Ir(III) complexes **3a**, **3e** and **3f** as either slow-acting or fast-acting compounds.[49] A synchronized, chloroquine-sensitive (NF54) strain of *P. falciparum* in ring phase at 2% haematocrit with 2% parasitemia was used to conduct this experiment. Four 96-well plates were set up for one biological replicate. The highest testing concentrations for **3a** and **3f** was 5 mg mL^{-1} and 10 mg mL^{-1} for **3e**. Chloroquine (CQ), artemisinin (ART) and ferroquine (FQ) were used as the controls. The blank contained 100 μL complete medium and 100 μL 2% haematocrit. A serial dilution was performed. Each plate represented a drug exposure time-point of 10, 24, 48 or 72 h. At each time-point, the corresponding plate was removed and the antimalarial compounds and controls were aspirated. Fresh complete medium (200 μL) was, thereafter, added to each well. All four plates were incubated at 37 °C for a total of 72 h. After 72 h, the parasite viability was assessed using a SYBR-green flow cytometry-based method. All the plates were removed, resuspended and the contents of each transferred to separate round-bottom plates, which were then centrifuged at 750 rpm for 5 min. The complete medium was then aspirated and the parasites were washed twice with 100 μL filtered PBS. A SYBR-green solution was made up by adding 1.00 μL SYBR-green into 10.0 mL of filtered PBS and, thereafter, 100 μL of this SYBR-green solution was added to each plate. The plates were then covered with foil and incubated at 37 °C for 1 hour. After incubation, a BD CSampler™ Plus Flow Cytometer was used to run these plates, with each well being run for 10 seconds on medium flow rate with one agitation every 12 wells in a cycle. The IC_{50} values obtained from each plate were then calculated as ratios relative to the IC_{50} value at 72 h. The following formula, with 72 h being the baseline IC_{50} value for each drug, was used:

$$IC_{50} \text{ of 10 or 24 or 48 h}/IC_{50} \text{ of 72 h} = IC_{50} \text{ relative to 72 h.}$$

β-Haematin inhibition assay

The β-haematin formation assay was modified from the method described by Sandlin *et al.*[50] The test compounds were prepared as 10 mM stock solutions in DMSO. The compounds were delivered to a 96-well plate in triplicate and were tested at a starting concentration of 1 mM, where the lowest drug concentration was 1 μM. The stock solution was serially diluted to give 11 concentrations in the 96-well flat-bottom assay plate. NP-40 detergent was then added to mediate the formation of β-haematin (30.55 μM, final concentration). A 25 mM stock solution of haematin was prepared by dissolving hemin (16.3 mg) in DMSO (1.00 mL). A 178 μL aliquot of haematin stock was suspended in 20 mL of a 2 M acetate buffer, pH 4.7. The haematin suspension was then added to the plate to give a final haematin concentration of 100 μM. The plate was then incubated for 16 h at 37 °C. The compounds were analysed using the pyridine-ferrochrome method developed by Ncokazi and Egan.[51] 32 μL of a solution of 50% pyridine, 20% acetone, 20% water, and 10% 2 M HEPES buffer (pH 7.4) was added to each well. To this, 60 μL acetone was then added to each well and mixed. The UV-Vis absorbance of the resulting complex was measured at 405 nm on a SpectraMax 340PC plate reader. The IC_{50} values were obtained using a non-linear dose–response curve fitting analysis *via* Graph Pad Prism v.5.0 software.

Transfer hydrogenation methods

Method for qualitative ^{1}H NMR spectroscopy study. Approximately 6.00 mg of the complex, 20.0 mg of NAD^+ and 40.0 mg of sodium formate were weighed. The NAD^+ was dissolved in 600 μL of D_2O and the sodium formate in 600 μL of MeOD, with sonication to aid in dissolving. The complex was then suspended in a mixture of 100 μL of the sodium formate solution and 300 μL of the NAD^+ solution. To this, 300 μL of MeOD was added. The suspension was then mixed well and any solid matter that remained was filtered off. The solution was then added to an NMR tube. The ^{1}H NMR spectrum was recorded prior to incubation at 37 °C. The tube was then incubated at 37 °C and the spectra recorded at various time intervals thereafter.

Method for cell-free assay to detect transfer hydrogenation of NAD^+ to NADH. A 50.0 mL solution containing NAD^+ at pH

7.4 was prepared as follows: sodium formate (0.310 g, 4.56 mmol), trizma base (0.330 g, 2.72 mmol) and NAD^+ (5.50 mg, 0.00829 mmol) were dissolved in 25.0 mL of distilled water. The pH was then adjusted to 7.4 using HCl. The volume was made up to 50.0 mL with distilled water. The tetrazolium solution (NBT) was prepared using nitroblue tetrazolium (NBT) (80.0 mg, 0.0978 mmol) and phenazine ethosulfate (4.00 mg, 0.0120 mmol) in 50.0 mL distilled water. 6 mM Stocks of each complex were prepared in DMSO (to 1.00 mL). In a 96-well plate, 200 μL of the drug solution was added in triplicate. 100 μL of DMSO was added to each well. The compounds were serially diluted giving 10 concentrations. 75.0 μL of the solution from each well was transferred into a second 96-well plate into the corresponding well (*e.g.* 75.0 μL C1 of plate 1 into C1 of plate 2 *etc.*). 100 μL of the NAD^+ solution was then added to each well. 75.0 μL DMSO and 100 μL NAD^+ solution were added to each well only. 175 μL DMSO was added to each well only. The plate was read at 600 nm to account for the absorbance of the compounds (pre-read). The plate was then covered with a foil plate cover to prevent evaporation and was incubated for 6–8 h at 37 °C. After this time, 25.0 μL of the NBT solution was added and the plate incubated for a further 24 h to aid plate developing. After this time, the absorbance was read at 600 nm again, the data from the pre-read accounted for and the data plotted using Graph Pad Prism v.5.0 at the various concentrations (2250 μM to 4 μM).

Conflicts of interest

There are no conflicts of interest to declare.

Acknowledgements

Financial support from the University of Cape Town, the National Research Foundation of South Africa (UID: 111707) and the Harry Crossley Research Fellowship is gratefully acknowledged. Dr Jill Combrinck and Ms Chiao-Yu (Zoey) Hsiao from the Department of Clinical Pharmacology (University of Cape Town) are also gratefully acknowledged for their assistance with the CHO cytotoxicity and IC_{50} speed assays.

References

1 M. Navarro, W. Castro and C. Biot, *Organometallics*, 2012, **31**, 5715–5727.
2 World Health Organization, *World Malaria Report 2018*, Geneva, 2018.
3 M. Foley and L. Tilley, *Clin. Pharmacol. Ther.*, 1998, **79**, 55–87.
4 R. Banerjee and D. E. Goldberg, in *Antimalarial Chemotherapy: Mechanisms of Action, Resistance, and New Directions in Drug Discovery*, Humana Press Inc, Totowa, NJ, 1st edn., 2001.
5 P. F. Salas, C. Herrmann and C. Orvig, *Chem. Rev.*, 2013, **113**, 3450–3492.
6 M. Navarro, W. Castro, M. Madamet, R. Amalvict, N. Benoit and B. Pradines, *Malar. J.*, 2014, **13**, 1–8.
7 World Health Organisation, *Guidelines for the Treatment of Malaria*, Geneva, 2006.
8 R. G. Ridley, *Nature*, 2002, **415**, 686–693.
9 N. Baartzes, T. Stringer and G. S. Smith, in *Advances in Bioorganometallic Chemistry*, ed. T. Hirao and T. Moriuchi, Elsevier, 2019, pp. 193–213.
10 E. M. Guantai, K. Ncokazi, T. J. Egan, J. Gut, P. J. Rosenthal, P. J. Smith and K. Chibale, *Bioorg. Med. Chem.*, 2010, **18**, 8243–8256.
11 G. M. Fisher, R. P. Tanpure, A. Douchez, K. T. Andrews and S. A. Poulsen, *Chem. Biol. Drug Des.*, 2014, **84**, 462–472.
12 N. Boechat, M. D. L. G. Ferreira, L. C. S. Pinheiro, A. M. L. Jesus, M. M. M. Leite, C. C. S. Júnior, A. C. C. Aguiar, I. M. De Andrade and A. U. Krettli, *Chem. Biol. Drug Des.*, 2014, **84**, 325–332.
13 X. M. Chu, C. Wang, W. L. Wang, L. L. Liang, W. Liu, K. K. Gong and K. L. Sun, *Eur. J. Med. Chem.*, 2019, **166**, 206–223.
14 S. Vandekerckhove and M. D'Hooghe, *Bioorg. Med. Chem.*, 2015, **23**, 5098–5119.
15 E. Tesfaselassie, *Antimalarial Drug Discovery using Triazoles to Overcome Chloroquine Resistance*, Portland, OR, 2000.
16 A. H. Kategaonkar, P. V. Shinde, A. H. Kategaonkar, S. K. Pasale, B. B. Shingate and M. S. Shingare, *Eur. J. Med. Chem.*, 2010, **45**, 3142–3146.
17 S. Manohar, S. I. Khan and D. S. Rawat, *Chem. Biol. Drug Des.*, 2011, **78**, 124–136.
18 M. S. Malik, S. A. Ahmed, I. I. Althagafi, M. A. Ansari and A. Kamal, *RSC Med. Chem.*, 2020, **11**, 327–348.
19 N. P. E. Barry and P. J. Sadler, *ACS Nano*, 2013, **7**, 5654–5659.
20 M. Navarro, C. Gabbiani, L. Messori and D. Gambino, *Drug Discovery Today*, 2010, **15**, 1070–1078.
21 G. Gasser and N. Metzler-Nolte, *Curr. Opin. Chem. Biol.*, 2012, **16**, 84–91.
22 C. S. Allardyce and P. J. Dyson, in *Bioorganometallic Chemistry. Topics in Organometallic Chemistry*, Springer, Berlin, Heidelberg, Vol. 17, 2006, pp. 177–210.
23 B. Rosenberg, *Cancer*, 1985, **55**, 2303–2316.
24 C. Biot, G. Glorian, L. A. Maciejewski, J. S. Brocard, O. Domarle, G. Blampain, P. Millet, A. J. Georges, H. Abessolo, D. Dive and J. Lebibi, *J. Med. Chem.*, 1997, **40**, 3715–3718.
25 C. Biot, F. Nosten, L. Fraisse, D. Ter-Minassian, J. Khalife and D. Dive, *Parasite*, 2011, **18**, 207–214.
26 A. Kondratskyi, K. Kondratska, F. V. Abeele, D. Gordienko, C. Dubois, R. A. Toillon, C. Slomianny, S. Lemière, P. Delcourt, E. Dewailly, R. Skryma, C. Biot and N. Prevarskaya, *Sci. Rep.*, 2017, **7**, 1–15.
27 S. A. Charman, S. Arbe-Barnes, I. C. Bathurst, R. Brun, M. Campbell, W. N. Charman, F. C. K. Chiu, J. Chollet, J. C. Craft, D. J. Creek, Y. Dong, H. Matile, M. Maurer,

J. Morizzi, T. Nguyen, P. Papastogiannidis, C. Scheurer, D. M. Shackleford, K. Sriraghavan, L. Stingelin, Y. Tang, H. Urwyler, X. Wang, K. L. White, S. Wittlin, L. Zhou and J. L. Vennerstrom, *Proc. Natl. Acad. Sci. U. S. A.*, 2011, **108**, 4400–4405.

28 To Evaluate the Efficacy of a Single Dose Regimen of Ferroquine and Artefenomel in Adults and Children With Uncomplicated Plasmodium Falciparum Malaria (FALCI), https://clinicaltrials.gov/ct2/show/NCT02497612, (accessed 20 October 2019).

29 Y. C. Ong and G. Gasser, *Drug Discovery Today: Technol.*, DOI: 10.1016/j.ddtec.2019.06.001.

30 T. Stringer, M. A. S. Quintero, L. Wiesner, G. S. Smith and E. Nordlander, *J. Inorg. Biochem.*, 2019, **191**, 164–173.

31 L. Rylands, A. Welsh, K. Maepa, T. Stringer, D. Taylor, K. Chibale and G. S. Smith, *Eur. J. Med. Chem.*, 2019, **161**, 11–21.

32 E. Ekengard, K. Kumar, T. Fogeron, C. de Kock, P. J. Smith, M. Haukka, M. Monari and E. Nordlander, *Dalton Trans.*, 2016, **45**, 3905–3917.

33 J. J. Soldevila-Barreda and N. Metzler-Nolte, *Chem. Rev.*, 2019, **119**, 829–869.

34 P. K. Sasmal, C. N. Streu and E. Meggers, *Chem. Commun.*, 2013, **49**, 1581–1587.

35 K. D. Mjos and C. Orvig, *Chem. Rev.*, 2014, **114**, 4540–4563.

36 Z. Yu and J. A. Cowan, *Chem. – Eur. J.*, 2017, **23**, 14113–14127.

37 S. Betanzos-Lara, Z. Liu, A. Habtemariam, A. M. Pizarro, B. Qamar and P. J. Sadler, *Angew. Chem., Int. Ed.*, 2012, **51**, 3897–3900.

38 J. J. Soldevila-Barreda, P. C. A. Bruijnincx, A. Habtemariam, G. J. Clarkson, R. J. Deeth and P. J. Sadler, *Organometallics*, 2012, **31**, 5958–5967.

39 J. J. Soldevila-Barreda, I. Romero-Canelón, A. Habtemariam and P. J. Sadler, *Nat. Commun.*, 2015, **6**, 6582.

40 T. Stringer, D. R. Melis and G. S. Smith, *Dalton Trans.*, 2019, **48**, 13143–13148.

41 F. Himo, T. Lovell, R. Hilgraf, V. V. Rostovtsev, L. Noodleman, K. B. Sharpless and V. V. Fokin, *J. Am. Chem. Soc.*, 2005, **127**, 210–216.

42 V. V. Rostovtsev, L. G. Green, V. V. Fokin and K. B. Sharpless, *Angew. Chem., Int. Ed.*, 2002, **41**, 2596–2599.

43 D. L. Davies, O. Al-duaij, J. Fawcett, M. Giardiello, S. T. Hilton and D. R. Russell, *Dalton Trans.*, 2003, **2**, 4132–4138.

44 Z. Liu, A. Habtemariam, A. M. Pizarro, S. A. Fletcher, A. Kisova, O. Vrana, L. Salassa, P. C. A. Bruijnincx, G. J. Clarkson, V. Brabec and P. J. Sadler, *J. Med. Chem.*, 2011, **54**, 3011–3026.

45 Q. Du, L. Guo, M. Tian, X. Ge, Y. Yang, X. Jian, Z. Xu, Z. Tian and Z. Liu, *Organometallics*, 2018, **37**, 2880–2889.

46 R. Hubel, K. Polborn and W. Beck, *Eur. J. Inorg. Chem.*, 1999, **1999**, 471–482.

47 J. N. Burrows, D. Leroy, J. Lotharius and D. Waterson, *Future Med. Chem.*, 2011, **3**, 1401–1412.

48 J. N. Burrows, R. Hooft van Huijsduijnen, J. J. Möhrle, C. Oeuvray and T. N. Wells, *Malar. J.*, 2013, **12**, 187.

49 C. Le Manach, C. Scheurer, S. Sax, S. Schleiferböck, D. Cabrera, Y. Younis, T. Paquet, L. Street, P. Smith, X. C. Ding, D. Waterson, M. J. Witty, D. Leroy, K. Chibale and S. Wittlin, *Malar. J.*, 2013, **12**, 424.

50 R. D. Sandlin, M. D. Carter, P. J. Lee, J. M. Auschwitz, S. E. Leed, J. D. Johnson and D. W. Wright, *Antimicrob. Agents Chemother.*, 2011, **55**, 3363–3369.

51 K. K. Ncokazi and T. J. Egan, *Anal. Biochem.*, 2005, **338**, 306–319.

52 Y. K. Yan, M. Melchart, A. Habtemariam, A. F. A. Peacock and P. J. Sadler, *J. Biol. Inorg. Chem.*, 2006, **11**, 483–488.

53 J. W. Kang, K. Moseley and P. M. Maitiis, *J. Am. Chem. Soc.*, 1969, **91**, 5970–5977.

54 *SAINT Version 7.60a*, Bruker AXS Inc., Madison, WI, USA, 2006.

55 G. M. Sheldrick, *SHELXS-97, SHELXL-2014 and SADABS version 2.05*, University of Göttingen, Germany, 2004.

56 L. J. Barbour, *J. Supramol. Chem.*, 2001, **1**, 189–191.

57 J. L. Atwood and L. J. Barbour, *Cryst. Growth Des.*, 2003, **3**, 3–8.

58 W. Trager and J. Jensen, *Science*, 1976, **193**, 673–675.

59 M. T. Makler and D. J. Hinrichs, *Am. J. Trop. Med. Hyg.*, 1993, **48**, 205–210.